Determination of the thermal neutron induced $^{41}Ca(n,p)^{41}K$ and $^{41}Ca(n,\alpha)^{38}Ar$ reaction cross sections

C. Wagemans
Department of Subatomic and Radiation Physics, University of Gent, Proeftuinstraat 86, B-9000 Gent, Belgium

R. Bieber and H. Weigmann
European Community, Joint Research Centre, Institute for Reference Materials and Measurements, Retieseweg, B-2440 Geel, Belgium

P. Geltenbort
Institute Laue-Langevin, Boite Postale 156, F-38042 Grenoble, France
(Received 30 June 1997)

The $^{41}Ca(n,p)^{41}K$ and $^{41}Ca(n,\alpha)^{38}Ar$ reaction cross sections were determined with thermal neutrons at the high flux reactor of the ILL in Grenoble. For the $^{41}Ca(n_{th},p)^{41}K$ reaction cross section, a value of (7 ± 2) mb was obtained. In the case of the $^{41}Ca(n_{th},\alpha)^{38}Ar$ reaction, the transition to the ground state in ^{38}Ar has a cross section $\sigma(n_{th},\alpha_0) = (42\pm6)$ mb, the most prominent decay going to the first excited state in ^{38}Ar with a cross section $\sigma(n_{th},\alpha_1) = (130\pm25)$ mb. This can be explained by the presence of a nearby bound level with $J^\pi = 4^-$. Also $^{41}Ca(n_{th},\gamma\alpha)^{38}Ar$ transitions have been observed with a cross section of (10 ± 2) mb. The primary γ transitions are shown to have a $M1$ multipolarity. [S0556-2813(98)02304-8]

PACS number(s): 25.40.Hs, 26.30.+k, 26.45.+h, 27.40.+z

I. INTRODUCTION

Neutron induced reactions on ^{41}Ca are interesting from a nuclear physics point of view as well as for astrophysics applications.

^{41}Ca is indeed one of the rare nuclides with positive reaction energies for both proton and α emission after thermal neutron capture, i.e., $Q_p = 1.20$ MeV and $Q_\alpha = 5.22$ MeV respectively [1]. Moreover, α decay is possible to the ground state (α_0) and to the first excited level (α_1) in ^{38}Ar and the large Q_α value facilitates the study of the two-step $(n,\gamma\alpha)$ decay, as schematically illustrated in Fig. 1.

From an astrophysics point of view, the $^{41}Ca(n,p)^{41}K$ and $^{41}Ca(n,\alpha)^{38}Ar$ reactions play an important role in the *s*-process nucleosynthesis of nuclides from S to Ca (see, e.g., Refs. [2,3]) and in the explanation of Ca/Ti anomalies in meteorites [4]. Although the most relevant cross sections in this respect correspond to neutron energies in the keV range, accurate thermal neutron induced cross-section values are often used for the normalization of the higher energy data. Moreover, their knowledge is also required when calculating Maxwellian averaged cross sections via a summation of the thermal and resonance contributions [5].

Since no experimental cross-section determinations were available for the $^{41}Ca(n_{th},p)^{41}K$ and $^{41}Ca(n_{th},\alpha)^{38}Ar$ reactions, we performed a series of dedicated measurements at the high flux reactor of the Institut Laue-Langevin in Grenoble, France. This undertaking was, however, seriously hampered by the rareness of enriched ^{41}Ca and problems associated with the production and assaying of the samples [6].

II. EXPERIMENTAL PROCEDURE

A. Experimental setup

The experiments were performed at the end of the 87 m curved neutron guide H22, which delivers a thermal neutron flux of about 5×10^8 neutrons/cm^2 s at the sample position. The ratio of slow neutrons to epithermal and fast neutrons is 10^6, and the direct γ-ray flux from the reactor is reduced by a factor 10^6, and so the background conditions are excellent.

The sample was mounted in a vacuum chamber together with a suited Si-Au surface barrier detector placed outside the neutron beam. The detector was calibrated by means of the well-known $^6Li(n_{th},\alpha)t$, $^{10}B(n_{th},\alpha)^7Li$, $^{14}N(n_{th},p)^{14}C$, and $^{143}Nd(n_{th},\alpha)^{140}Ce$ reactions.

For the flux determination the Ca sample was replaced by an accurately defined U sample, strictly maintaining the detection geometry. So the $^{41}Ca(n_{th},p)$ and $^{41}Ca(n_{th},\alpha)$ cross sections were determined relative to the $^{235}U(n_{th},f)$ cross section, for which a value of (584.25 ± 1.10) b was adopted as recommended in the ENDF-B6 nuclear data file.

B. Sample characteristics

A variety of samples were used, all prepared by the Sample Preparation Group of the IRMM in Geel, Belgium. Initially, only $CaCO_3$ with an enrichment in ^{41}Ca of 1.33% was available. Later on, some carbonate with a ^{41}Ca enrichment of 63.38% could be obtained. In both cases, samples were produced via suspension spraying of the material on 20-μm-thick Al backings covering an area of 5×6 cm^2 (this corresponds to the beam profile seen by a sample mounted under an angle of 30°). It turned out that the initial mass determination of these samples via differential weighing was unreliable due to adsorption of water and other impurities by the material, a phenomenon which was not expected with $CaCO_3$ [6]. Finally, a small amount of $CaCO_3$ with an enrichment in ^{41}Ca of 81.69% could be obtained. This material was transformed into CaF_2 before spraying, which resulted in a water-free sample with a good energy resolution.

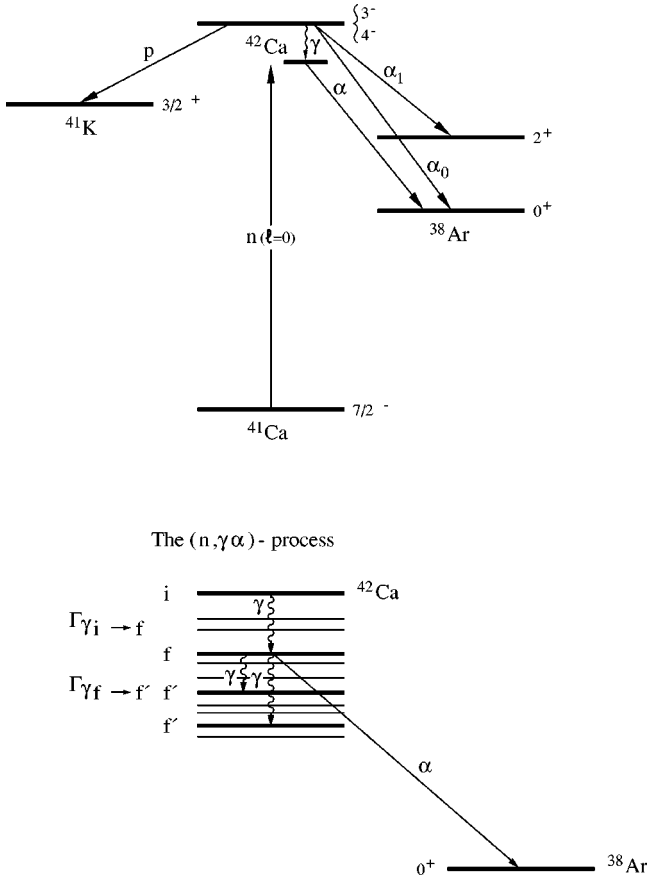

FIG. 1. Schematic representation of the decay of the compound nucleus ^{42}Ca via charged particle emission. The lower part illustrates the two-step $(n,\gamma\alpha)$ process, i, f, and f' being different ^{42}Ca compound states.

For the final mass determination, the differential weighing method was abandoned and substituted by a nuclear method based on the detection of the 3.3 keV K x rays emitted during the decay of ^{41}Ca. The same method has been used for the assaying of ^{37}Ar samples and is described in [7].

The accuracy of the number of ^{41}Ca atoms in the layer deduced from the count rate of the K x rays depends on the characteristics of the electron capture (EC) decay of ^{41}Ca. For the electron capture probability P_K a value of 0.896 ± 0.004 was used and a fluorescence yield ω_K equal to 0.144 ± 0.004 was adopted [8]. The major source of uncertainty is, however, the half-life of ^{41}Ca. Based on the results reported by Paul *et al.* [9], a conservative value of $(1.06\pm 0.10)\times 10^5$ y was deduced [8].

For the final measurements, a thin $^{41}CaF_2$ sample was used (enrichment 81.69%), with a total ^{41}Ca mass of (23 ± 3) μg. A few additional measurements were performed with a thicker $CaCO_3$ sample (enrichment 63.38%) containing (289 ± 37) μg of ^{41}Ca.

C. Measurements

1. $^{41}Ca(n_{th},\alpha)^{38}Ar$ measurements

For the very first experiments, a 450 mm^2 in area and 100-μm-thick Si-Au surface barrier detector was used. The $^{41}Ca(n_{th},\alpha_0)$ transition ($E_\alpha = 4.73$ MeV) could already be observed during tests with the 1.33% enriched ^{41}Ca sample

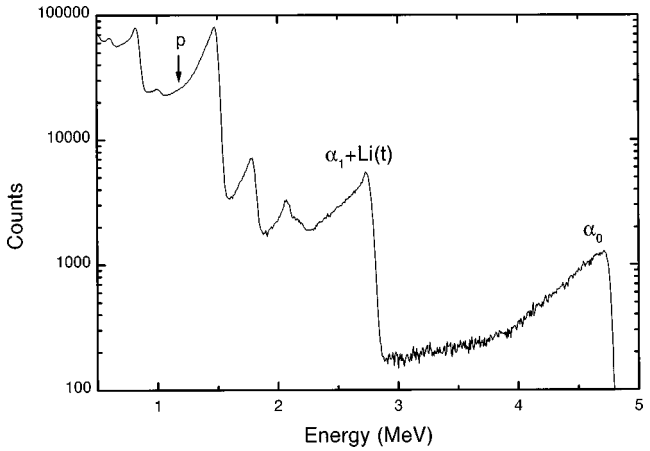

FIG. 2. Energy distribution of the reaction products obtained by bombarding a 63.38% enriched $^{41}CaCO_3$ sample with thermal neutrons.

[6]. The prominence of this transition became obvious in the measurements with the 63.38% enriched sample, as shown in Fig. 2. This figure also illustrates the poor energy resolution due to the impurities in the layer mentioned above. It furthermore shows that the $^{41}Ca(n_{th},\alpha_1)$ particles ($E_\alpha = 2.76$ MeV) are mixed up with 2.72 MeV tritons from $^6Li(n_{th},\alpha)t$ reactions and that the 1.2 MeV protons from the $^{41}Ca(n_{th},p)^{41}K$ reaction are completely drown in a sea of $^{10}B(n_{th},\alpha)^7Li$ reaction products (respectively due to ^{6}Li and ^{10}B impurities in the sample). From these measurements it became clear that improved detection conditions were needed to permit a clean detection of the α_1 particles and the protons.

For the final $^{41}Ca(n_{th},\alpha_0)$ measurements, the sample with 81.69% enrichment was used, in combination with a 300 mm^2 in area and 28-μm-thick totally depleted Si-Au detector with a resolution of 50 keV. With this detector thickness, the tritons are not completely stopped and no longer mixed up with the α_1 particles. A typical spectrum is shown in Fig. 3, which also illustrates the improved energy resolution as compared to Fig. 2. The intrinsic energy resolution of the detection chain is illustrated in Fig. 4, which shows a calibration spectrum obtained with a thin ^{10}B sample (1 μg of ^{10}B evaporated on a 1 cm^2 Al foil). The slight low-energy tailing observed for the α_0 and α_1 lines in Fig. 3 is due to the poorer resolution of the $^{41}CaF_2$ sample, which was prepared via suspension spraying. This effect however hardly disturbs the $(n,\gamma\alpha)$ region.

Figure 3 also reveals the presence of several lines in between the α_0 and α_1 transitions, which we interpret as evidence for $^{41}Ca(n_{th},\gamma\alpha)$ transitions (see Sec. III).

In all cases, background measurements were performed with the sample mounted but without neutrons, with the sample rotated over 180°, and with a dummy sample (neutron beam on in both cases).

2. $^{41}Ca(n_{th},p)^{41}K$ measurements

For these measurements a 300 mm^2 in area and 30-μm-thick totally depleted Si-Au detector was used, covered, however, with a 5-μm-thick Mylar foil. Thanks to the difference in energy loss between α particles and protons, the $^{41}Ca(n_{th},p)$ transition can be observed under these circumstances, as shown in Fig. 5.

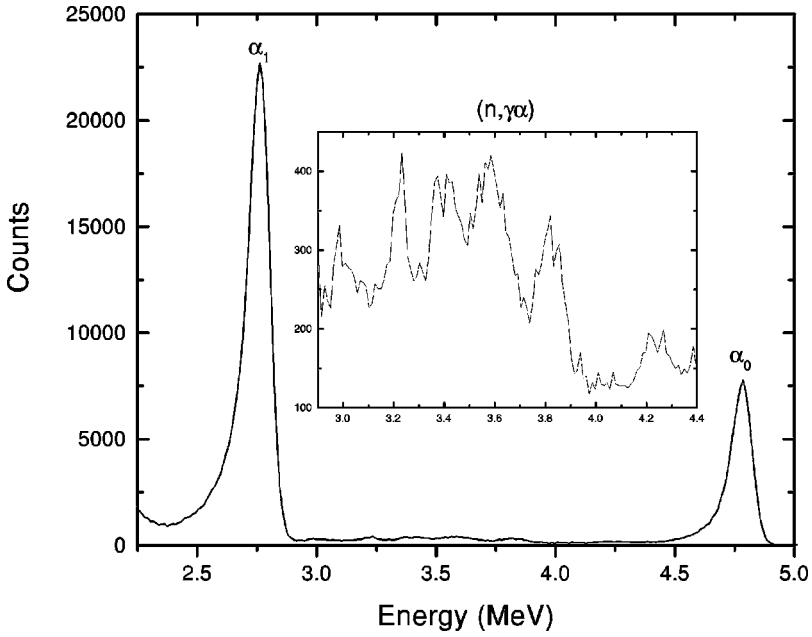

FIG. 3. Energy distribution of the ^{41}Ca$(n_{\rm th},\alpha)$ particles obtained with a 81.69% enriched $^{41}CaF_2$ sample, using a 28-μm-thick detector.

III. RESULTS AND DISCUSSION

The cross-section values are calculated by means of the following expression:

$$\sigma(\mathrm{Ca}) = \frac{N(^{235}\mathrm{U})}{N(^{41}\mathrm{Ca})}\,\frac{C(^{41}\mathrm{Ca})}{C(^{235}\mathrm{U})}\,\sigma_f(^{235}\mathrm{U}), \qquad (1)$$

in which N is the number of atoms per cm^2, C the counting rate after background substraction of the respective reactions, and $\sigma_f(^{235}\mathrm{U})$ the thermal neutron induced fission cross section of ^{235}U.

For the $(n_{\rm th},\alpha)$ cross sections, the following results were obtained:

(i) ^{41}Ca$(n_{\rm th},\alpha_0)^{38}$Ar (42 ± 6) mb,

(ii) ^{41}Ca$(n_{\rm th},\alpha_1)^{38}$Ar (130 ± 25) mb.

In both cases, the (1σ) uncertainty is mainly determined by the uncertainty in the number of ^{41}Ca atoms in the layer.

Surprisingly, the probability for the transition to the first excited level in ^{38}Ar is much larger than that of the ground state transition. We will interpret this result based on the schematic level scheme given in the upper part of Fig. 1. After the capture of an s-wave neutron ($l = 0$) in ^{41}Ca, excited ^{42}Ca levels with a spin and parity $J^\pi = 3^-$ or 4^- are formed. From a 3^- level , α transitions to 0^+ ($l_\alpha=3$) as well as to 2^+ levels ($l_\alpha=1$) are permitted; in other words, α_0 as well as α_1 particles can be emitted. This is, however, not the case for a 4^- level which can only α decay ($l_\alpha=3$) to the 2^+ level, the $4^- \rightarrow 0^+$ transition being parity forbidden. In other words, only α_1 but no α_0 particles can be emitted from a 4^- resonance.

We calculated the corresponding α-particle penetrabilities with the optical model routine CERBERO [10], using the α-particle potential parameters of Huizenga and Igo [11]. This calculation shows that from a 3^- initial state the partial α decays to the ground state ($l_\alpha=3$) and to the 2^+ excited state ($l_\alpha=1$) are expected to have an intensity ratio of about 400 instead of the observed one of 0.32. Of course, actual transition probabilities may differ strongly from expected ones due to Porter-Thomas fluctuations, but a factor of 1200 between expected and observed ratios is rather improbable.

The observed $\sigma(n_{\rm th},\alpha_0) < \sigma(n_{\rm th},\alpha_1)$ thus indicates that a strong 4^- resonance or bound level should be present near the thermal energy region. Since no sufficiently strong low-energy resonances were observed [12], the existence of a nearby bound level is needed to explain the observed result.

As shown in Fig. 3, we also observed several ^{41}Ca$(n_{\rm th},\gamma\alpha)$ transitions with a clear peak structure at about a 200 keV interval and an all over cross section of (10 ± 2) mb. Here, the error is about equally determined by the uncertainty in the number of ^{41}Ca atoms and that on the background correction.

In the lower part of Fig. 1 we take a closer look at the two-step $(n,\gamma\alpha)$ process. This rather rare phenomenon has, so far, only be investigated in detail for ^{40}K and ^{143}Nd [13,14] and it permits one to obtain unique experimental information on low-energy radiative transitions between two compound states (indicated by i and f in Fig. 1).

Figure 6 shows a transformation of the experimental

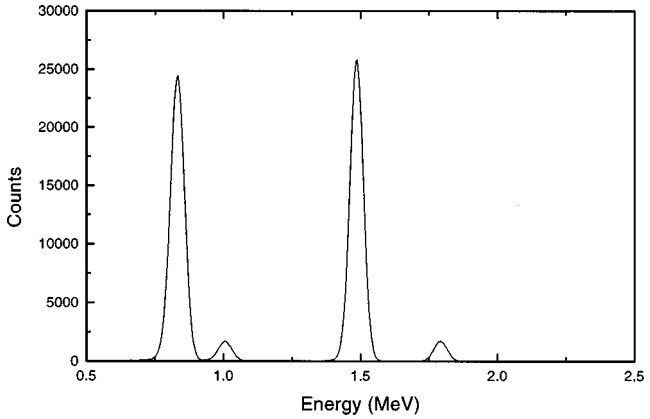

FIG. 4. Energy calibration of the 28-μm-thick Si-Au detector with the ^{10}B$(n_{\rm th},\alpha_0)^7$Li and ^{10}B$(n_{\rm th},\alpha_1\gamma)^7$Li* reactions yielding calibration peaks at 0.830 MeV (^{7}Li*), 1.007 MeV (^{7}Li), 1.483 MeV (α_1), and 1.789 MeV (α_0).

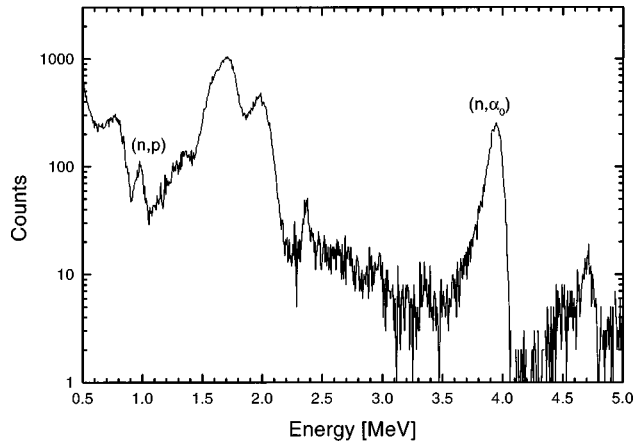

FIG. 5. Energy distribution of the reaction products obtained by bombarding a 81.69% enriched $^{41}CaF_2$ sample with thermal neutrons, using a 30-μm-thick detector covered with 5 μm of Mylar.

$^{41}Ca(n_{th},\gamma\alpha)$ data (after background correction) displayed in the inset of Fig. 3. The dots are obtained by replacing the α energy by the corresponding energy of the primary γ ray, followed by averaging the data over 80 keV energy bins. The curves are the spectral shapes calculated under various assumptions and normalized to the maximal experimental yield. The spectral shape $W\gamma\alpha(E\gamma)$ was calculated as follows:

$$W\gamma\alpha(E\gamma)\approx\Gamma\gamma_{i\to f}\rho\frac{\Gamma\alpha_{f\to 0}}{\Gamma\alpha_{f\to 0}+\Gamma\gamma_{f\to f'}}, \qquad (2)$$

$\Gamma\gamma_{i\to f}$ being the width for γ decay from level i (corresponding to the compound state populated by thermal neutron capture) towards a level f at energy $E_x=B-E_\gamma$; $\Gamma\alpha_{f\to 0}$ and $\Gamma\gamma_{f\to f'}$ are the widths of level f for α decay to the ground state and γ decay to all lower levels f'; ρ is the level density at energy E_x.

In order to calculate the spectral shape for transitions of type $E1$ ($l_\alpha=4$) and $M1$ ($l_\alpha=3$), $\Gamma\gamma_{i\to f}\approx E_\gamma^3$ (i.e., the single-particle Weisskopf estimate) was substituted in relation (2). Whereas the total calculated $(n,\gamma\alpha)$ yields for the combination $E1$ ($l_\alpha=4$) and $M1$ ($l_\alpha=3$) were about equal, the yield for the combination $E1$ ($l_\alpha=3$) was smaller by a factor of $\approx$700 and may thus be ignored.

It is clear that the best agreement with the experimental data is obtained assuming a predominant $M1$ multipolarity of the primary radiation [15].

One could at first glance be surprised that neighboring (compound) nuclei such as ^{42}Ca and ^{41}K [13] reveal such different multipolarities, i.e., $M1$ and $E1$ respectively. This can, however, be explained by their specific spectroscopic properties.

Indeed, in the case of ^{42}Ca the thermal cross section appears to be dominated by a 4^- state. So $M1$ transitions may lead to 3^- which can decay ($l_\alpha=3$) to the ground state. $E1$ transitions on the other hand would have to go via 4^+ and $l_\alpha=4$. Optical model calculations show that $\Gamma_{\alpha_0}(l_\alpha=3)/\Gamma_{\alpha_0}(l_\alpha=4)\approx 3$, which clearly favors $M1$ transitions.

The situation is quite different for ^{41}K, where the thermal cross section is dominated by a $7/2^-$ state. Here $E1$ transitions lead to $5/2^+$, $7/2^+$, and $9/2^+$, of which the first two may decay ($l_\alpha=3$) to the ground state of ^{37}Cl ($3/2^+$). $M1$ transitions on the other hand populate $5/2^-$, $7/2^-$, and $9/2^-$ states, of which only $5/2^-$ may decay ($l_\alpha=1$) to the ground state.

For the $^{41}Ca(n_{th},p)^{41}K$ reaction cross section finally, a value of (7 ± 2) mb was determined. Also in this case, the error is about equally determined by the uncertainty in the number of ^{41}Ca atoms and that in the background correction (see Fig. 5).

These thermal reaction cross sections can be used for the normalization of corresponding experiments with higher-energy neutrons and combined with these to calculate Maxwellian averaged cross sections. Moreover, the presently determined thermal cross-section values are fairly large and

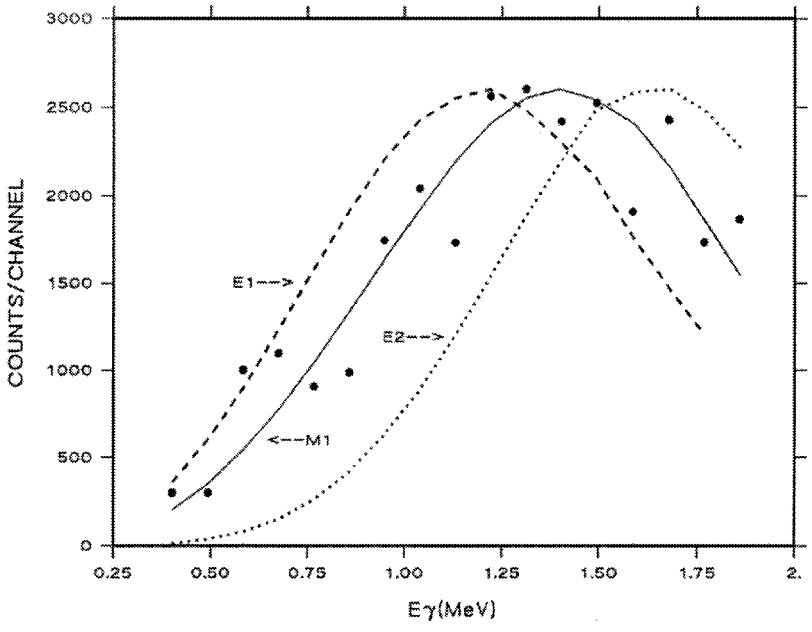

FIG. 6. Experimental (dots) and calculated (curves) spectral shapes for the $^{41}Ca(n_{th},\gamma\alpha)$ transitions; the curve for $E2$ ($l_\alpha=3$) has been multiplied by a factor of $\approx$700 for display.

indicate that the *s*-process nucleosynthesis path is likely to be influenced by ^{41}Ca(n,α) and ^{41}Ca(n,p) reactions.

IV. CONCLUSIONS

In the present work the ^{41}Ca$(n_{\rm th},\alpha)^{38}$Ar and ^{41}Ca$(n_{\rm th},p)^{41}$K reaction cross sections were determined for the first time. Besides a fairly strong ^{41}Ca$(n_{\rm th},\alpha_0)$ transition, a dominant ^{41}Ca$(n_{\rm th},\alpha_1)$ line was observed, indicating that a strong 4^- bound state should be present near the thermal energy region. Furthermore, evidence was found for significant ^{41}Ca$(n_{\rm th},\gamma\alpha)$ transitions with a $M1$ multipolarity of the primary γ rays.

[1] P. Endt, Nucl. Phys. **A521**, 1 (1990).

[2] M. Sevior, M. Anderson, L. Mitchell, S. Kennett, and D. Sargood, Nucl. Phys. **A378**, 349 (1982).

[3] H. Beer and R. Penzhorn, Astron. Astrophys. **174**, 323 (1987).

[4] K. Takahashi and W. Hillebrandt, in Proceedings of the 7th Workshop on Nuclear Astrophysics, Ringberg Castle (D), Report No. MPA/P7 99, 1993 (unpublished).

[5] Z. Bao and F. Käppeler, At. Data Nucl. Data Tables **36**, 411 (1987).

[6] C. Wagemans, Nucl. Instrum. Methods Phys. Res. A **282**, 4C (1989).

[7] C. Wagemans, M. Loiselet, R. Bieber, B. Denecke, D. Reher, and P. Geltenbort, Nucl. Instrum. Methods Phys. Res. A **397**, 22 (1997).

[8] D. Reher and B. Denecke (private communication).

[9] M. Paul, I. Ahmad, and W. Kutschera, Z. Phys. A **340**, 249 (1991).

[10] F. Fabbri, G. Fratamico, and G. Reffo, CNEN Report No. RT/Ti(77)6, 1977.

[11] J. Huizenga and G. Igo, Nucl. Phys. **29**, 462 (1962).

[12] C. Wagemans *et al.* (unpublished).

[13] A. Emsallem, M. Asghar, C. Wagemans, and H. Weigmann, Nucl. Phys. **A368**, 108 (1981).

[14] N. Balanov, V. Vtyurin, Y. Gledenov, and Y. Popov, Sov. J. Part. Nucl. **21**, 131 (1990).

[15] C. Wagemans, P. Schillebeeckx, H. Weigmann, and S. Druyts, in *Proceedings of the 8th International Symposium on Capture Gamma-Ray Spectroscopy and Related Topics*, Fribourg (Switzerland), edited by J. Kern (World Scientific, London, 1994), p. 638.